# Metric-Driven RoSy Fields Design

Yu-Kun Lai[1], Miao Jin[2], Xuexiang Xie[3], Ying He[3],
Jonathan Palacios[4], Eugene Zhang[4], Shi-Min Hu[1] and Xianfeng David Gu[2]

Technical Report **TR-080201**
Tsinghua University, Beijing, China

[1] Department of Computer Science and Technology, Tsinghua University, Beijing, China.
[2] Department of Computer Science, Stony Brook University, Stony Brook, NY, USA.
[3] School of Computer Engineering, Nanyang Technological University, Singapore.
[4] School of Electrical Engineering and Computer Science, Oregon State University, Corvallis, OR, USA.

# Metric-Driven RoSy Fields Design

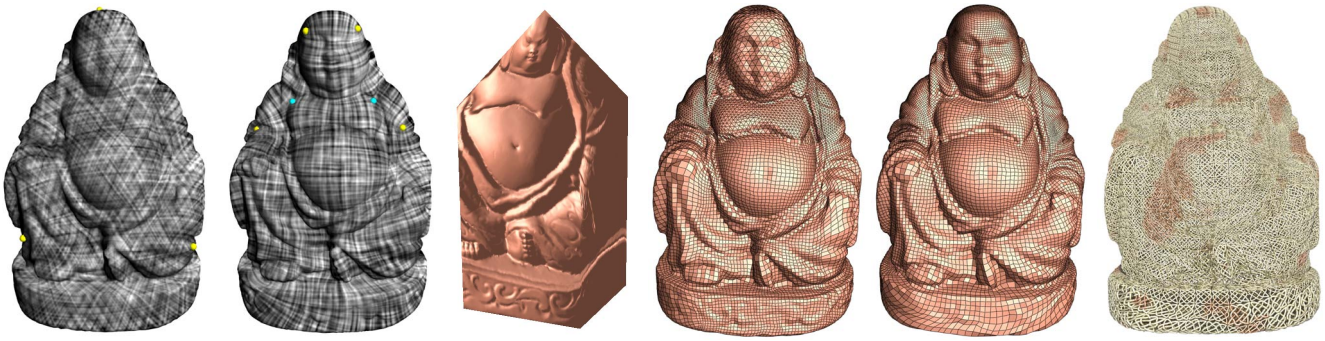

**Figure 1:** *Metric-driven N-RoSy field design. From left to right, a 3-RoSy field, a 4-RoSy field, a flat cone metric visualized as an obelisk, triangle-quad mixed remeshing based on the metric, quad-remeshing, woven Celtic knot design over the surface based on the quad-remeshing.*


## Abstract

Designing rotational symmetries on surfaces is an important task for a wide range of graphics applications. This work introduces a rigorous and practical algorithm for automatic N-RoSy design on arbitrary surfaces with user defined field topologies. The user has full control of the number, positions and indices of the singularities, the turning numbers of the loops, and is able to edit the field interactively.

We formulate N-RoSy field construction as designing a Riemannian metric, such that the global symmetry of the metric is compatible with the local symmetry of N-RoSy. We prove the compatibility condition using discrete parallel transportation.

The complexity of N-RoSy field design is caused by curvatures. In our work, we propose to simplify the Riemannian metric to make it flat almost everywhere. This approach greatly simplifies the process and improves the flexibility, such that, it can design N-RoSy fields with single singularity, and mixed-RoSy. This approach can also be generalized to construct regular remeshing on surfaces.

To demonstrate the effectiveness of our approach, we apply our design system to pen-and-ink sktetching and geometry remeshing. Furthermore, based on our remeshing results with high global symmetry, we generate Celtic knots on surfaces directly.



**CR Categories:** I.3.5 [Computer Graphics]: Computational Geometry and Object Modeling—Geometric algorithms, languages, and systems; I.3.5 [Computer Graphics]: Computational Geometry and Object Modeling—Curve, surface, solid, and object representations

**Keywords:** metric, rotational symmetry, design, surface


## 1 Introduction

Many objects in computer graphics and digital geometry processing can be described by *rotational symmetries*, such as brush strokes and hatches in non-photorealistic rendering, regular patterns in texture synthesis, and principle curvature directions in surface parameterizations and remeshing. N-way rotational symmetry (N-RoSy) has been proposed to model these objects.

The most important requirement for an N-RoSy field design system is to allow the user to fully control the topology of the field, including the number, positions and indices of the singularities, and the turning numbers of the loops [Palacios and Zhang 2007; Ray et al. to appear]. Automatic generation of N-RoSy fields with user prescribed topologies remains a major challenge.

The method in [Palacios and Zhang 2007] generates fields with user defined singularities, but it also produces excess singularities, which requires further singularity pair cancellation and singularity movement operations. The method in [Ray et al. to appear] is the first one that guarantees the correct topology of the field, but it requires the user to provide an initial field with all singularities at the desired positions. In practice, finding such an initial field is the most challenging step. For example, a common user can hardly imagine a smooth vector with only one singularity as shown in Figure 8 and Figure 2. Whereas fields with less singularities are often preferred, because singularities cause visual artifacts in real applications.

In this work, we provide a rigorous and practical method which allows the user to design N-RoSy fields with full control of the topology and without inputting any initial field. Furthermore, the algorithm can automatically generate a smooth field with the desired topology and allow the user to further modify it interactively.

### 1.1 Main Idea

Our method is based on the following intuition inspired by the work in [Ray et al. to appear]. An N-RoSy field has *local symmetry* that is invariant under rotations of an integer multiple of $\frac{2\pi}{N}$. A surface has *global symmetry*, which is intrinsically determined by the Riemannian metric. If the global symmetry is *compatible* with the N-RoSy symmetry, then smooth N-RoSy fields can be constructed on the surface directly.

Roughly speaking, if a surface admits an N-RoSy field, then for any loop on the surface the total turning angle of the tangent vectors along the loop cancels the total turning angle of the N-RoSy field along the loop. Figure 7 provides such an example where a genus one polycubic surface admits 4-RoSy fields.

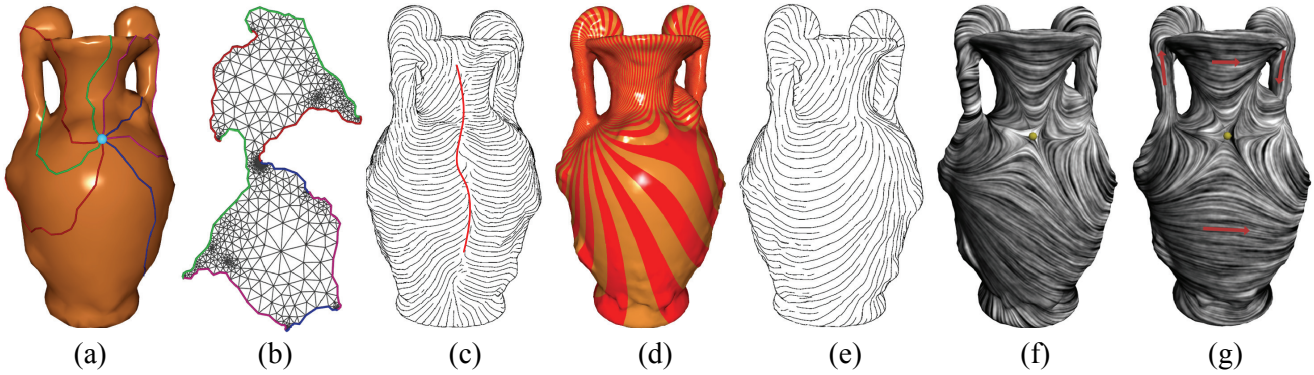


**Figure 2: Algorithm pipeline** *(a). User specifies the desired singularities with both positions and indices. Here one singularity at the blue point with the index* $-2$*. The curves are homotopy group basis. (b) We compute a flat metric, the curvature at the singularity is* $-4\pi$*, everywhere else* $0$*. The surface is cut along the base curves and flatten to the plane. Note that the boundaries of the same color can match each other by a rigid motion. (c) Parallel vector field. The field has discontinuities along the red curve. (d) Compute a harmonic 1-form to compensate the holonomy. (e) The smooth vector field after rotation compensation. (f)(g) User inputs geometric constraints (red arrows) to guide the direction of the field, then the field is modified from (f) to (g).*

Most existing N-RoSy design methods focus on adjusting the rotation of the field and keep the underlying surface untapped. While these approaches have been effective in some cases, it is difficult to enforce topological guarantees such as minimal number of singularities. Furthermore, these methods all require a constant N in the N-RoSy fields. In this paper, we describe a novel approach that modifies both the rotation of the field and the rotations of the loops by deforming the surface.

This approach greatly simplifies the process and produces results that are quite challenging for the alternatives, such as mixed-RoSy and remeshing in Figure 1, as well as fields with only one singular point in Figure 2 and 8.

### 1.2 Algorithm Pipeline

Our algorithm pipeline can be summarized as follows. In the first stage, an initial smooth vector field is constructed with the following steps: 1. the user specifies the desired singularities of the vector field; 2. we compute a flat cone metric, such that all the cone singularities coincide with those of the field; 3. we parallel transport a tangent vector at the base point to construct a parallel vector field; 4. if the parallel field has jumps when it goes around handles or circulates singularities, we apply two methods to eliminate the jumps: *rotation compensation* adjusts the rotation of the vector field; *metric compensation* modifies the rotation of the loops by deforming the surface. In the second stage, the vector field is further modified. we interactively edit the rotation and the magnitude of the vector field to incorporate user constraints. Figure 2 illustrates the pipeline using rotation compensation method.

### 1.3 Contributions

In this work, *holonomy* plays the central role, which refers to the total turning angle of the tangent vectors along a loop. Holonomy represents the global symmetry of the surface.

This work introduces a metric-driven method for N-RoSy design (and re-meshing). The major goal is to make the global symmetry of the metric represented as holonomy to be compatible with the local symmetry of N-RoSy field.

- We convert the N-RoSy field design problem (and remeshing problem) to flat cone metric design with constrained holonomy, and propose to use flat cone metric to simplify holonomy and improve the efficiency and efficacy of the algorithm. Furthermore, we give an explicit compatibility condition for a parallel N-RoSy field with the metric and generalize it for symmetric tessellations.
- We give rigorous and practical algorithms to construct N-RoSy fields with user fully controlled singularities on general surfaces. The method produces RoSy fields with arbitrary homotopy types, without excess singularities, and even with mixed-RoSy types. The algorithm is automatic and interactive.

Furthermore, we apply our remeshing method for the geometric texture synthesis application to construct knotwork on general surfaces, which requires highly global symmetries.

Note that, this work focuses on the design and manipulation of metrics, it has the potential to be utilized for other graphics applications.

The organization of the paper is as follows. In Section 2, we briefly review the most related works. In Section 3 we give a brief introduction of the major concepts in Riemannian geometry and generalize them to discrete surfaces, and describe the theories for the compatibility between N-RoSy and metric. In Section 4, we explain the algorithm in detail. Finally we report our experimental results in Section 5 and conclude in Section 6 with insights and future directions of research. All the proofs of our theoretic results can be found in the appendix.

## 2 Previous Work

There has been a significant amount of work in the analysis and design of N-RoSy fields, especially when $N = 1$(vector) and 2(tensor). For a survey, we refer the readers to Palacios and Zhang [2007] and references therein. Here, we will only mention the most relevant work.

There have been a number of vector field design systems for surfaces, most of which are generated for a particular graphics application such as texture synthesis [Praun et al. 2000; Turk 2001; Wei and Levoy 2001], fluid simulation [Stam 2003], and vector field visualization [van Wijk 2002; van Wijk 2003]. Systems providing topological control include [Theisel 2002; Zhang et al. 2006]. The system of Zhang et al. has also been extended to create periodic orbits [Chen et al. 2007] and to design tensor fields [Zhang et al. 2007]. Fisher et al. introduce a vector field design algorithm based on discrete exterior calculus [Fisher et al. 2007], which produces smooth fields incorporating user constraints interactively through weighted least squares.

There has been some work on N-RoSy fields when $N > 2$. Hertz-

mann and Zorin [2000] and Ray et al. [2006] demonstrate that 4-RoSy fields are of great importance in surface illustration and remeshing, respectively. Both works also develop algorithms that can smooth the 4-RoSy fields in order to reduce the noise in the fields. Later, Ray et al. [to appear] provide the analysis of singularities on N-RoSy's by by extending the Poincaré-Hopf theorem as well as describe an algorithm in which a field with a minimal number of singularities can be constructed based on user-specified constraints and the Euler characteristic of the underlying surface [Ray et al. to appear]. This is the first algorithm that performs provably correct direction field design. Palacios and Zhang provide comprehensive analysis for rotational symmetry fields on surfaces and present efficient algorithms for locating singularities, separatrices, and effective design operations in [Palacios and Zhang 2007].

### 2.1 Pen-and-ink Sketching of Surfaces

Pen-and-ink sketching of surfaces is a non-photorealistic style of shape visualization. The efficiency of the visualization and the artistic appearance depend on a number of factors, one of which is the direction of hatches. Girshick et al. [2000] show that 3D shapes are best illustrated if hatches follow principle curvature directions. However, curvature estimation on discrete surfaces is a challenging problem. While there have been several algorithms that are theoretically sound and produce high-quality results [Hertzmann and Zorin 2000; Meyer et al. 2002; Cohen-Steiner and Morvan 2003; Rusinkiewicz 2004], most of them still rely on smoothing to reduce the noise in the curvature estimate. Consequently, these methods do not provide control over the singularities in the field. Hertzmann and Zorin [2000] propose the concept of cross fields, which are 4-RoSy fields obtained from the curvature tensor (a 2-RoSy field) by removing the distinction between the major and minor principle directions. They demonstrate that smoothing on the cross field tends to produce more natural hatch directions than smoothing directly on the curvature tensor. They also point out the need to control the number and location of the singularities in the field. Zhang et al. [2007] address this issue by providing singularity pair cancellation and movement operations on the curvature tensor field. However, their technique cannot handle a 4-RoSy field.

### 2.2 Texture synthesis

In [Wei and Levoy 2001], 2 and 4-symmetry direction fields are used to steer synthesizing using 2 and 4-symmetry texture samples. [Zelinka and Garland 2004] steer their texture generation method using a direction field defined as the gradient of a fair Morse function (it has the same singular points as the function). Based on the study of the Morse complex of smooth harmonic functions [Ni et al. 2004], this allows a user-controllable number and configuration of singularities. The gradient of the harmonic function is a direction field. The first work on computer generated Celtic knot was introduced by Kaplan and Cohen in [Kaplan and Cohen 2003]. [Zhou et al. 2006] introduces mesh quilting method for geometric texture synthesis through local stitching and deformation. Our method for constructing Celtic knots on surfaces is a global method without partitioning the surface and stitching the texture patches.

### 2.3 Quad-Dominant Remeshing

The problem of quad-dominant remeshing, i.e., constructing a quad-dominant mesh from an input mesh, has been a well-studied problem in computer graphics. The key observation is that a nice quad-mesh can be generated if the orientations of the mesh elements follow the principle curvature directions [Alliez et al. 2003]. This observation has led to a number of efficient remeshing algorithms that are based on streamline tracing [Alliez et al. 2003; Marinov and Kobbelt 2004; Dong et al. 2005]. Ray et al. [2006] note that better meshes can be generated if the elements are guided by a 4-RoSy field. They also develop an energy functional that can be used to generate a periodic global parameterization and to perform quad-based remeshing. The connection between quad-dominant remeshing and 4-Rosy fields has also inspired Tong et al. [2006] to generate quad meshes by letting the user design a *singularity graph* that resembles the behavior of the topological skeleton of a 4-RoSy field. On the other hand, Dong et al. [2006] perform quad-remeshing using spectral analysis, which produces quad meshes that in general do not align with the curvature directions. A seminal method is introduced in [Kälberer et al. 2007], which converts a 4-RoSy field on a surface to a vector field by using 4 layer branched covering.

### 2.4 Metric Design

Kharevych et al. used circle patterns for discrete conformal mappings in [Kharevych et al. 2006]. The Euclidean flat cone metric with user prescribed singularities can be obtained by two stage optimizations. Jin et al. used circle packing to design flat cone metrics in [Jin et al. 2007], which handles spherical, Euclidean and hyperbolic discrete metrics. The algorithm is the discrete analogy of Ricci flow [Hamilton 1982]. A linear metric scaling method for computing Euclidean flat cone metric with prescribed curvatures is introduced in [Ben-Chen et al. 2008], where the cone singularities can be automatically selected to minimize the distortion. Circle pattern and discrete Ricci flow are non-linear methods, requires a preprocessing stage, and get an accurate metric; the metric scaling method is linear and flexible for general meshes but with less accuracy.

## 3 Theoretic Foundations

In this section, we first briefly introduce Riemannian geometry theories, and then generalize them to discrete settings. Next we present our major theoretical results. The detailed proofs can be found in the Appendix.

### 3.1 Basic Concepts in Riemannian Geometry

In order to quantitatively measure the rotation of a vector field along a curve and the rotation of curve itself on a surface, we need to introduce some tools from Riemannian geometry. **Parallel transportation** on a curved surface plays the central role. Suppose $\gamma$ is a curve on the surface $S$. The envelope of all the tangent planes along $\gamma$ is a developable surface $\tilde{S}$, we develop the envelope to the plane, $\gamma$ becomes a planar curve. Suppose $\mathbf{v}$ is a tangent vector at a point $p$, we translate it to $\tilde{\mathbf{v}}$ on the plane along the development of $\gamma$. This corresponds to the parallel transportation on the surface. The angle between the resulting transported vector and the initial vector is called the rotational component of the **holonomy** along $\gamma$, or simply the holonomy of $\gamma$. Holonomy describes the global symmetry of the surface. Figure 3 illustrates a parallel transportation on a sphere $S$, where $\gamma$ is a circle, $\tilde{S}$ is a conic surface, angle $\theta$ is the holonomy along $\gamma$.

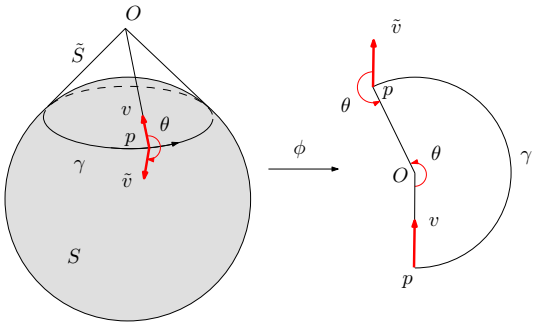


**Figure 3:** *Parallel transport and holonomy. $\theta$ is the holonomy along $\gamma$.*

Suppose a vector field $\mathbf{v}$ (in red) is along a path $\gamma$, connecting $p$

and $q$. We parallel transport the tangent vector at the starting point $p$ to the ending vertex $q$, this parallel vector field is $\mathbf{w}$ in blue. The rotation $\theta$ between from $\mathbf{w}(q)$ to $\mathbf{v}(q)$ is called the *absolute rotation* of the vector field $\mathbf{v}$ along the path $\gamma$. The absolute rotation of the tangent direction of $\gamma$ is equal to its holonomy. The *relative rotation* of the vector field $\mathbf{v}$ along the path $\gamma$ is the difference between the absolute rotation of $\mathbf{v}$ and the holonomy of $\gamma$, which indicates the change of the angle between $\mathbf{v}$ and the tangent vector of $\gamma$ along $\gamma$. The **compatibility condition** for a smooth N-RoSy field on a surface is that for any loop $\gamma$, the relative rotation of $\mathbf{v}$ along $\gamma$ is an integer times of $\frac{2\pi}{N}$. Our central task is to make the absolute rotation of a vector field and the holonomy to cancel out each other.

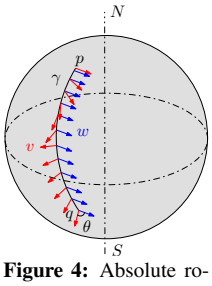

**Figure 4:** Absolute rotation.

Parallel transportation and holonomy along loops on curved surfaces are very complicated, which contributes to the difficulty of N-RoSy design. For example, if $\gamma$ is the boundary of a surface patch $\Omega$, then the holonomy of $\gamma$ equals to the total curvature on $\Omega$, $\int_\Omega K$, where $K$ is the Gaussian curvature. Therefore, the parallel transportation is path dependent. If $K$ is zero everywhere, namely, the surface is flat, then parallel transportation is path independent. The surface global symmetry is extremely easy to analyze. Unfortunately, according to the Gauss-Bonnet theorem, the total Gaussian curvature of the surface is a constant $2\pi\chi(S)$, where $\chi(S)$ is the Euler characteristic number of the surface. If the surface is not of genus one, then its Riemannian metric cannot be flat everywhere.

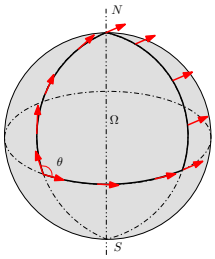

**Figure 5:** Holonomy vs. curvature.

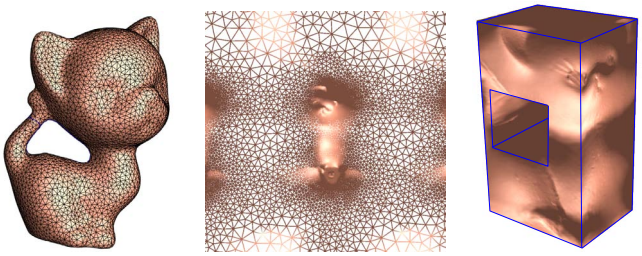
**Figure 6:** *Flat cone metrics on a genus one kitten mesh. The first metric has no cone singularities, the second metric has* 16 *cone singularities, i.e.corners of polycube.*

Fortunately, we can design a **flat cone metric** of an arbitrary surface, such that the curvature is zero almost everywhere except at finite number of cone singularities. Let $\mathbf{g}$ be the induced Euclidean metric tensor on $S$. Suppose a user has selected the position and curvatures of the singularities on a surface, the target curvature is $\bar{K}$, then the target metric can be deformed by the Hamilton's surface Ricci flow [Hamilton 1982], $\frac{d\mathbf{g}(t)}{dt} = (\bar{K} - K_{\mathbf{g}(t)})\mathbf{g}(t)$. Figure 6 demonstrates two different flat cone metrics of a genus one surface obtained by using Ricci flow.

### 3.2 Discrete Theories

All the aforementioned Riemannian geometric concepts are defined on smooth surfaces. In the following, we generalize the major concepts to the discrete settings.

Let $M$ be a triangular mesh in $\mathbb{R}^3$. A *metric* of $M$ is a configuration of edge lengths, such that the triangular inequality holds on all faces. The *vertex curvature* is the angle deficit, i.e., $2\pi$-the total angle around the vertex. A *flat cone metric* is a metric such that the curvatures are zero for almost all the vertices, except at a few ones. The vertices with non-zero curvatures are called the *cone singularities*. Note that metric determines curvatures. Reversely, given the curvatures on vertices, we can uniquely determine a metric using the methods in [Kharevych et al. 2006; Jin et al. 2007; Ben-Chen et al. 2008]. Figure 6 shows two flat cone metrics for a genus one kitten model. The mesh is developed onto the plane by a flat metric without singularities. While the curvature is determined by the metric, the total curvature of the surface is determined by the topology of the mesh, which is equal to $2\pi\chi(M)$, where $\chi(M)$ is the Euler characteristic number.

Let $M$ be a mesh with a flat cone metric, and $S = \{s_1, s_2, \cdots, s_n\}$ be the cone singularity set. Let $\bar{M}$ denote the mesh obtained by removing all the cone singularities from $M$, $\bar{M} = M \backslash S$.

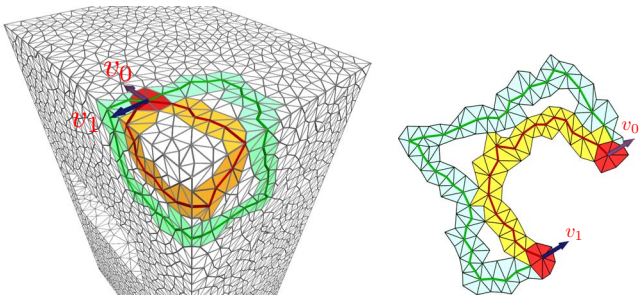

**Figure 7:** *Discrete parallel transportation and holonomy. Homotopic loops sharing the base vertex have the same holonomy.*

**Parallel Transport** Parallel transportation is the direct generalization of planar translation. Let $\gamma$ be a path consisting of a sequence of consecutive edges on $\bar{M}$, the sorted vertices of $\gamma$ are $\{v_0, v_1, \cdots, v_n\}$. Let $N_i$ denote the one-ring neighborhood of $v_i$ (the union of all the faces adjacent to $v_i$), then the one-ring neighborhood of $\gamma$ is defined as the union of all $N_i$'s: $N(\gamma) = \bigcup_{i=0}^{n} N_i$.

The *development* of $N(\gamma)$ refers to the following process: first we flatten $N_0$ on the plane, and then we extend the flattening to $N_1$, such that the common faces in both $N_0$ and $N_1$ coincide on the plane. This process is repeated until $N_n$ is flattened. In this way, we develop $N(\gamma)$ to the plane. We denote the development map as $\phi : N(\gamma) \to \mathbb{R}^2$. Note that the restriction of the development map on each triangle is a planar rigid motion. *Parallel transportation* on the mesh along $\gamma$ is defined as the translation on the development of $N(\gamma)$. See Figure 7 for the illustration of parallel transportation.

**Holonomy** In practice, we are more interested in the *loop* case, i.e. $v_0 = v_n$. When parallel transporting a tangent vector at $v_0$ along $\gamma$ to $v_n$, the resulting vector differs from the original vector by a rotation, which is the *holonomy* of the loop, denoted as $h(\gamma)$. Given a vector field $\mathbf{v}$ along $\gamma$, we parallel transport the vector at the starting point. The vector at the ending point differs from the transported vector, which is the *absolute rotation* of the field along $\gamma$, denoted as $R_{\mathbf{v}}(\gamma)$.

Two loops $\gamma_1, \gamma_2$ sharing a base point $p$ are *homotopic*, if one can deform to the other. The concatenation of $\gamma_1, \gamma_2$ through $p$ is still a loop, which is the product of them. All homotopy classes of loops form a group, the so-called homotopy group $\pi(\bar{M})$. Suppose $M$ has $g$ handles, and $n$ cone singularities. Then the basis of $\pi(\bar{M})$ is depicted in Figure 9, where each handle has two loops $a_k, b_k$, and each singularity $s_i$ has one loop $c_i$. Details are explained in [Ray et al. to appear].

Homotopic loops have the same holonomy if the underlying surface has a flat cone metric. In this case, we can define the *holonomy map*,

$h : \pi(\bar{M}) \rightarrow SO(2)$, where $SO(2)$ is the rotation group in the plane. Its image $h(\pi(\bar{M}))$ is the *holonomy group* of $M$, denoted as $holo(\bar{M})$.

**Compatibility N-RoSy** The *relative rotation* of a vector $\mathbf{v}$ along $\gamma$ is defined as the difference of the absolute rotation of $\mathbf{v}$ and the holonomy of $\gamma$, $T_{\mathbf{v}}(\gamma) = R_{\mathbf{v}}(\gamma) - h(\gamma)$. The relative rotation is equivalent to the *turning number* defined by [Ray et al. to appear]. Ray et al. proved that for a smooth N-RoSy field, the turning number along any loop must be integer times of $\frac{2\pi}{N}$.

$$T_{\mathbf{v}}(\gamma) = R_{\mathbf{v}}(\gamma) - h(\gamma) \equiv 0, mod \frac{2\pi}{N}. \quad (1)$$

Furthermore, the turning numbers on a basis of the homotopy group $\pi(\bar{M})$

$$\{T_{\mathbf{v}}(a_1), T_{\mathbf{v}}(b_1), \cdots, T_{\mathbf{v}}(a_g), T_{\mathbf{v}}(b_g), T_{\mathbf{v}}(c_1), \cdots, T_{\mathbf{v}}(c_n)\} \quad (2)$$

determine the homotopy class of the N-RoSy field. We develop our theoretical results based on these fundamental facts. All the proofs are given in the appendix.

The following theorems lay down the theoretical foundation of our metric-driven method, which claims that the topological properties of a vector field are preserved by metric deformation.

**Theorem 3.1** *Suppose $\mathbf{v}$ is a smooth vector field on a surface $M$. $\mathbf{g}(t)$ is a one parameter family of Riemannian metric tensors. Then for any closed loop $\gamma$ on $M$, the relative rotation $T_{\mathbf{v}}(\gamma)$ on $(M, \mathbf{g}(t))$, i.e. $M$ with the metric $g(t)$, is constant for any $t$.*

The simplest N-RoSy field is the parallel field, the following theory leads us to design our algorithm.

**Theorem 3.2** *Suppose $M$ is a surface with a flat cone metric. A parallel N-RoSy field exists on the surface, if and only if all the holonomic rotation angles of the metric are integer times of $\frac{2\pi}{n}$.*

For genus zero closed surfaces, the curvature of cone singularities determine the holonomy.

**Corollary 3.3** *Suppose $M$ is a genus zero closed surface with finite cone singularities. $M$ has a parallel N-RoSy field, if and only if the curvature for each cone singularity is $\frac{2k\pi}{N}$.*

According to this corollary, it is easy to verify the symmetry of platonic solids. If a platonic solid has $N$ vertices, then the vertex curvature is $\frac{4\pi}{N}$, therefore the rotational homology group is generated by the rotation of angle $\frac{4\pi}{N}$, a $\frac{N}{2}$-RoSy field exists on it. For example, an octahedron is with 6 vertices and 3-RoSy; a dodecahedron is with 20 vertices and 10-RoSy.

The following existence theorem gurantees the existence of N-RoSy fields on surfaces with arbitrary flat cone metrics.

**Theorem 3.4** *Suppose $M$ is a surface with flat cone metric, then there exists a smooth N-RoSy field.*

Suppose $\tilde{M}$ is a branch covering of $M$ (defined in [Kälberer et al. 2007]), then the holonomy group of $\tilde{M}$ is a subgroup of that of $M$, $\tilde{M}$ may have more N-RoSy fields with lower $N$. For example, in [Kälberer et al. 2007], $M$ has a parallel 4-RoSy field, its 4-layer branch covering $\tilde{M}$ allows a parallel 1-RoSy field, namely, a vector field.

**Tessellation** We wish to generalize planar tessellation to general surfaces. If the symmetry of the metric on the surface is compatible with the symmetry of the planar tessellation, then the surface can be re-meshed according to the planar tessellation.

We generalize holonomy to include both translation and rotation. Figure 7 shows the concept. Given a loop $\gamma$, the starting vertex $v_1$ coincides with the ending vertex $v_n$, we develop its neighborhood $N(r)$ onto the plane, then the development of $N_1$ and that of $N_n$ differs by a planar rigid motion, which is defined as the *general holonomy* along $\gamma$. Two loops sharing the common base vertex share the same general holonomy. Therefore, general holonomy maps the homotopy group to a subgroup of planar rigid motion $E(2)$. We denote the image as $Holo(\bar{M})$, and call it the *general holonomy group* of $\bar{M}$.

Suppose $T$ is a tessellation of the plane $\mathbb{R}^2$, $\tau$ is a rigid motion preserving $T$, $\tau(T) = T$. The *symmetry group* of $T$ is defined as

$$G_T = \{\tau \in E(2) | \tau(T) = T\}.$$

**Theorem 3.5** *Suppose $M$ is with a flat cone metric, the holonomy group of $\bar{M}$ is $Holo(\bar{M})$, if $Holo(\bar{M})$ is a subgroup of $G_T$, then $T$ can be defined on $M$.*

# 4 Algorithm

Suppose the user specifies topological and geometric constraints for the N-RoSy field: *topological constraint* means the singularities, including the number, positions and indices; *geometric constraint* means the directions and lengths of the fields at some regions on the surface.

Our algorithm has two major stages: stage one is to compute an initial N-RoSy field, which satisfies the topological constraints; stage two is to edit the N-RoSy field, locally rotate and scale the initial field to satisfy the geometric constraints.

## 4.1 Initializing N-RoSy Field

This stage has 3 steps: compute the metric, compute the holonomy, and holonomy compensation. For genus zero meshes, we only need the first step, because the metric will be compilable with N-RoSy fields automatically according to corollary 3.3.

### 4.1.1 Computing the Flat Cone Metric

The cone singularities are fully determined by the singularities on the desired N-RoSy field. Let $v$ be a cone singularity, then its curvature and its index are closely related by the formula $Ind(v) = \frac{k(v)}{2\pi}$, where $Ind(v)$ is the index of $v$. If the index is non-positive, then it is easy to define the curvature of $v$. For vertex with a positive index, it is more complicated to find the curvature. We handle this situation in the following way. We punch a small hole at the cone singularity. Suppose the boundary vertices of the small hole are $\{v_1, v_2, \cdots, v_m\}$. Then the index of the singularity and the total curvature of the boundary are related by $Ind(v) = \frac{\sum_{i=1}^{m} k_i}{2\pi} + 1$. Given the desired curvature, we can compute a flat metric using one of the conventional methods. Figure 8 illustrates a vector field constructed using this method on the Michelangelo's David head surface,which is a genus zero closed surface, with one singularity of index $+2$.

According to corollary 3.3, the flat cone metrics on a genus zero closed mesh satisfy the compatible condition automatically. Figure 10 shows one example, both 3-RoSy and 4-RoSy fields on a genus zero surface are constructed by parallel transportation on the flat cone metric directly.

### 4.1.2 Computing the holonomy

For genus zero closed meshes, if the cone singularity curvatures satisfy the compatibility condition 1, then the flat cone metric of the surface satisfies the same condition. For high genus meshes, the cone singularity curvatures cannot guarantee the holonomy compatibility. Explicit computation is required, as shown by the following example on a genus three surface.

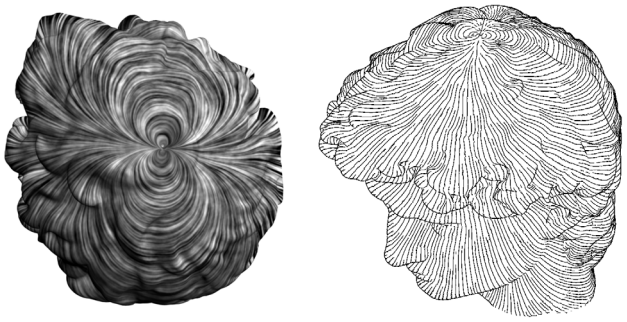

**Figure 8:** *A vector field on a genus zero closed surface with a single singularity with index* $+2$.

We compute a basis of the homotopy group $\pi(\bar{M})$ using the method in [Kälberer et al. 2007]. The base loops are shown in Figure 9. Then we compute the development of each base loop $\gamma$ to obtain the holonomy $h(\gamma)$. The holonomies of all the base loops form the generators of the holonomy group. For example, Figure 9 shows a genus three mesh with four cone singularities, which are labeled with different colors. The curvatures of the red, orange and blue singularities are $-\pi$,$-3\pi$,$-2\pi$, respectively. The holonomic rotation angles for $c_1$,$c_2$,$c_3$ are 0,$\pi$ and 0 (modulo $2\pi$).

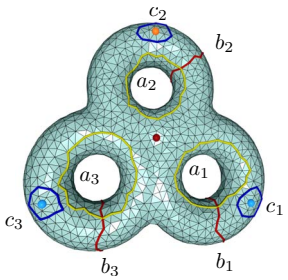


**Figure 9:** Homotopy basis for a 3-hole torus with 4 singularities.

The holonomic rotation angles (with respect to a modulus of $2\pi$) are as follows:

| $a_1$ | $b_1$ | $a_2$ | $b_2$ | $a_3$ | $b_3$ |
|---|---|---|---|---|---|
| $1.5551\pi$ | $0.9683\pi$ | $1.3704\pi$ | $1.5175\pi$ | $1.5975\pi$ | $1.0574\pi$ |

#### 4.1.3 Holonomy Compensation

There are two methods for holonomy compensation, rotation compensation and metric compensation. The first one is to adjust the absolute rotation of the direction field $R_{\mathbf{v}}(\gamma)$; the second one modifies the metric to change the holonomy $h(\gamma)$, such that the relative rotation is equal to $\frac{2k\pi}{N}$ along arbitrary loops.

**Rotation Compensation** This method is similar to the method in Ray et al. [to appear]. The rotation angle of the field is represented as a closed 1-form. The key difference is that, their method further rotates an existing *smooth* field and change the topology of the field; our method rotates a *non-smooth* field and make it smooth, it can also be applied to change the topology of a non-smooth field.

The homotopy class of the N-RoSy field is determined by the relative rotations on the basis of homotopy group in equation 2. We use a conventional method to compute a harmonic 1-form $\omega$ on $\bar{M}$, such that for any homotopy group generator $\gamma$, the following condition holds: for N-RoSy field design,

$$\int_{\gamma} \omega = T_{\mathbf{v}}([\gamma]) - h([\gamma]),$$

such a harmonic 1-form exists and is unique. Conceptually, the tangent field corresponding to the 1-form $\omega$ is constructed in the following way. We select a tangent vector $w_0$ at the base vertex. Suppose $v$ is another vertex, the shortest path on $\bar{M}$ from $v_0$ to $v$ is $\gamma$, then we parallel transport $w_0$ to $v$ along $\gamma$ to obtain $w$, then we rotate $w$ clock-wisely about the normal by an angle $\theta = \int_{\gamma} \omega$. By this way, we propagate the tangent vector $w_0$ to cover the whole mesh.

In practice, we use an equivalent fast marching method to propagate the vector field.
1. Select a tangent vector $w_0$ at $v_0$, put $v_0$ in a queue.
2. If the queue is empty, stop. Otherwise, pop the head vertex $v_i$ of the queue. Go through all the neighbors of $v_i$. For each neighboring vertex $v_j$, which hasn't been accessed, parallel transport $w_i$ from $v_i$ to $v_j$, rotate it counter-clock-wisely by angle $\omega(v_i, v_j)$. Enqueue $v_j$.
3. Repeat step 2, until all the vertices have been processed.
Figure 2 illustrates a vector field on a genus two amphora model with one singularity.

**Metric Compensation** For designing smooth N-RoSy fields, automatic rotation compensation is already enough. For the purpose of remeshing, metric compensation method will be required. In contrast to rotation compensation, this approach modifies the flat cone metric to achieve the desired general holonomy which satisfies the compatibility condition in Theorem 3.5.

Conventional algorithms [Kharevych et al. 2006; Jin et al. 2007; Ben-Chen et al. 2008] for flat cone metrics cannot produce metrics satisfying the holonomy constraint in Eqn.1. We observe that the flat cone metric on a polycube [Tarini et al. 2004] satisfies the compatibility condition in Eqn.1 for 4-RoSy fields. The flat metric on a mesh with all faces are equilateral triangles is compatible with 6-RoSy fields.

The following algorithm computes the desired flat cone metric for genus zero surfaces.
1. First, the user specifies the singularities of the N-RoSy field for both positions and indices, such that the curvatures satisfy the holonomy condition in Eqn.1 and are positive. Furthermore, the user specifies the connectivity of a polyhedron $P$, whose vertices are the cone singularities, and faces are either quadrilaterals or tri-

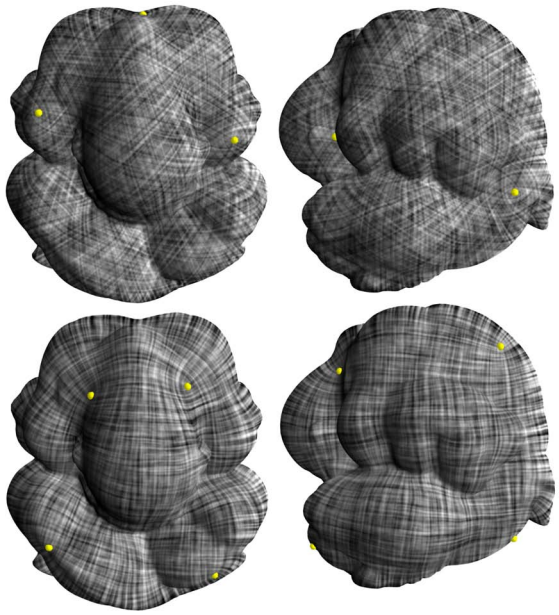

**Figure 10:** *The Pensatore surface is a genus zero closed mesh. A 3-RoSy field is shown in the first row, where there are* 6 *cone singularities with the curvatures of* $\frac{2\pi}{3}$. *A 4-RoSy field is shown in the second row, there are* 8 *cone singularities with the curvatures of* $\frac{\pi}{2}$.

angles.
2. We use the discrete Ricci flow method [Jin et al. 2007] to compute a flat cone metric. If $\{s_i, s_j\}$ is an edge in $P$, we compute the shortest path connecting $s_i, s_j$ under the flat metric. $P$ becomes a convex polyhedron.
3. We use Alexandrov embedding method in [Bobenko and Izmestiev 2007] to embed $P$ in $\mathbb{R}^3$.
4. We adjust the positions of all the vertices of $P$ to make the general holonomy of $P$ to satisfy the condition in Theorem 3.5.
For high genus surfaces, we apply polycube map method in [Tarini et al. 2004].

Figure 1 illustrates several remeshing results based on the metric compensation.

### 4.2 N-RoSy field Editing

Suppose users add some geometric constraints to the N-Rosy field, our method can incorporate them easily. We decompose the constraints as orientation constraints and length constraints. Suppose user specify the directions of the vectors at special point set $\omega \subset M$. Let $p \in \omega$, the angle between $\mathbf{w}(p)$ and the desired direction is $\psi(p)$. Then we compute a harmonic function using the method described in [Ni et al. 2004], $\psi : M \to \mathbb{R}$ with the boundary condition on $\Omega$. Then at each point $q \in M$, we rotate $\mathbf{w}(q)$ by an angle $\psi(q)$. The length constraint can be satisfied using the similar harmonic function method. Figure 11 demonstrate a vector field editing process on the kitten surface, the red arrows are specified directions, the vector field is modified to follow these directions interactively.

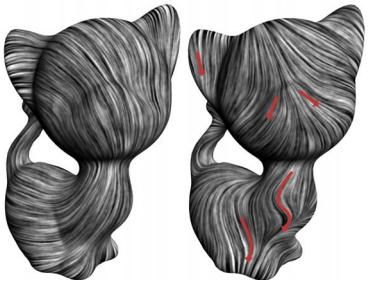

**Figure 11:** Vector field editing.

## 5 Experimental Results

We implemented our algorithm in C++ on an Intel Core2Duo 2GHz Laptop with 2GB memory. We report the timings for the major steps in Table 1, which include the computations for the flat metric, rotational compensation, and user editing. The flat metric computation accounts for most of the time, which can be taken offline. The rotation compensation and feedback to editing can be performed at an interactive rate. Also, if no user editing is involved, the whole pipeline is fully automatic.

**Remeshing** In the holonomy compensation step of stage one (section 4.1.3), we use the metric compensation method to adjust the metric to satisfy the tessellation compatibility condition in Theorem 3.5. Then we develop the mesh to the plane, and tessellate the development. This induces a desired tessellation.

**Table 1:** *Running times for different steps of our algorithm. (F-No. of faces, g-genus, s- No. of singularities)*

| Model | $F$ | $g$ | $s$ | Metric(s) | Comp.(s) | Edit(s) |
|---|---|---|---|---|---|---|
| kitten | 19350 | 1 | 0 | 100 | 0.078 | 0.410 |
| amphora | 20078 | 2 | 1 | 169 | 0.266 | 0.452 |
| venus | 20308 | 0 | 5 | 126 | 0.087 | 0.453 |
| bimba | 22412 | 0 | 6 | 67 | 0.098 | 0.522 |
| 3holes | 3514 | 3 | 4 | 4 | 0.157 | — |
| Pensatore(3-RS) | 21304 | 0 | 6 | 28 | 0.079 | — |
| Pensatore(4-RS) | 21304 | 0 | 8 | 25 | 0.083 | — |
| Buddha(3-RS) | 20828 | 0 | 6 | 10 | 0.078 | — |

Figure 1 demonstrates the results of N-RoSy field on the buddha model. Frame (a) and (b) show a 3-RoSy field and a 4-RoSy field on the buddha model respectively. In frame (c), a flat cone metric deforms the mesh in the shape of an obelisk, which induces a mixed 4-RoSy and 3-RoSy field on the mesh. (d) shows a mixed quadrilateral and triangle tessellation based on the flat cone metric. The Celtic knot in the last frame is constructed based on the quad-remeshing in frame (e).

**Celtic Knot on Surface** Celtic knot refers to a variety of endless knots, which in most cases contain delicate symmetries and entangled structures. Figure 12 shows a simple Celtic knot. To the best of our knowledge, Kaplan and Cohen [2003] were the first to present a technique for computer generated Celtic design. Most of their results focused on planar Celtic knot design, whereas our work emphasizes Celtic knots on surfaces with highly global symmetry.

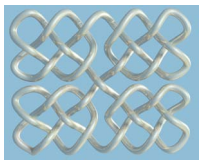

**Figure 12:** A planar Celtic knot.

The local symmetry and the quality of remeshing of the surfaces play crucial roles for the knotwork on surfaces. Based on our remeshed results, those uniform quads and triangles provide a perfect canvas for Celtic knot design. Similar to the method in [Kaplan and Cohen 2003], we set control points directly on surfaces, connecting them using polynomials based on the knot designing rules. Compared with traditional geometric texture synthesis approaches, we do not need shell mapping from planar domains to surfaces. Figures 1,13,16 show our Celtic knots synthesis results on several surfaces. The knotwork has complicated structures and rich symmetries.

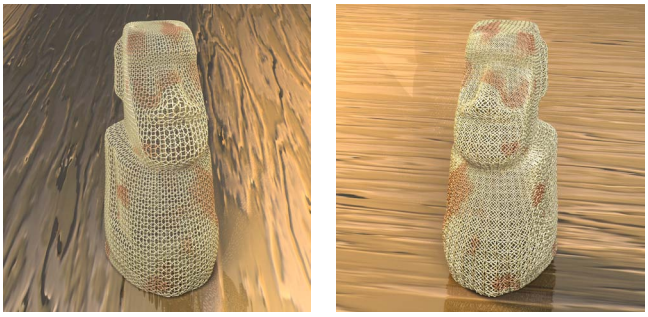

**Figure 13:** *Two woven Celtic knot designs on the Moai surface, which have different global symmetries.*

**Pen-and-ink Sketching of Surfaces** Pen-and-ink sketching of surfaces is a non-photorealistic style of shape visualization. In this work, we follow Hertzmann and Zorin [2000] by treating hatch directions as a 4-RoSy field.

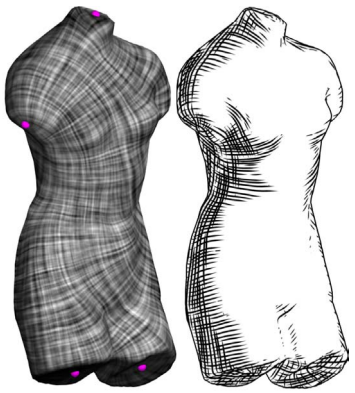

**Figure 14:** Pen-and-ink sketching.

Our method neither requires the user to input an initial field, nor generates excess singularities except those specified by the user. It enables the user to fully control the number, positions and the indices of singularities, and edit the field interactively. These merits make our system rather desirable for NPR applications.

For example, we perform the pen-and-ink sketching on the Venus

model in Figure 14 and Bimba model in Figure 15. The left columns show the 4-RoSy fields with user specified singularities, 6 for Bimba, 5 for Venus. Comparing with the algorithm in [Palacios and Zhang 2007], our method reduces the number of singularities by one order of magnitude, and locates them at the natural positions. This greatly reduces the visual artifacts and simplifies the designing process. The editing process improves the hatching quality on the Bimba model shown in 15.

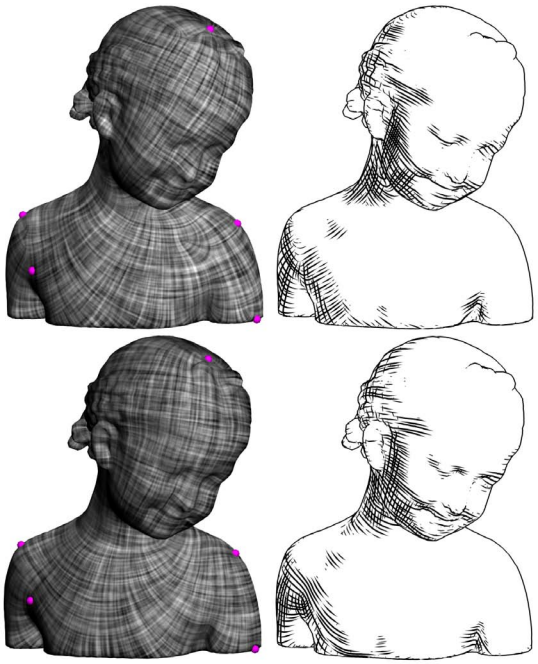

**Figure 15:** *Pen-and-ink sketching of bimba before (top row) and after editing (bottom row). The hatch directions follow the natural directions better (e.g. neck,arm).*

More experimental results are reported in our supplementary video and images.

## 6 Conclusion

This work introduces rigorous and practical algorithms for automatic N-RoSy field design on arbitrary surfaces with prescribed topologies. The user has full control of the number, positions and indices of the singularities, as well as the turning numbers of the loops.

We have also proved the compatibility condition between the metric and N-RoSy fields (and regular tessellation). Based on the theoretical findings, we turn the problem of N-RoSy field design to a metric design problem with constrained holonomy. By changing the metric of the surface, we enforce the global symmetry of the surface to be compatible with the local symmetry of the N-RoSy field. By using the flat cone metric, we greatly reduce the complexity of the design process. We also generalize the method for tessellation and mixed N-RoSy design.

We applied our algorithm for NPR rendering, remeshing, and geometric texture synthesis. We develop a global approach to design Celtic knot on surfaces.

Metric design is a very general approach, and we believe that it has potential of being applied for many other graphics tasks, such as parameterizations, mesh editing, and efficient rendering, etc. Our work demonstrates the effectiveness of using flat cone metrics to produce high quality N-RoSy fields. We also conjecture N-RoSy fields can be utilized to produce a special flat cone metric. In the future, we will explore further in these directions.

## References


ALLIEZ, P., COHEN-STEINER, D., DEVILLERS, O., LÉVY, B., AND DESBRUN, M. 2003. Anisotropic polygonal remeshing. *ACM Trans. Graph. 22*, 3 (July), 485–493.

BEN-CHEN, M., GOTSMAN, C., AND BUNIN, G. 2008. Conformal flattening by curvature prescription and metric scaling. *Comp. Graph. Forum 27*, 2.

BHAT, P., INGRAM, S., AND TURK, G. 2004. Geometric texture synthesis by example. In *Proc. Symp. Geom. Proc.*, 43–46.

BOBENKO, A. I., AND IZMESTIEV, I. 2007. Alexandrov's theorem, weighted delaunay triangulations, and mixed volumes. *arXiv:math0609447v1*.

CHEN, G., MISCHAIKOW, K., LARAMEE, R. S., PILARCZYK, P., AND ZHANG, E. 2007. Vector field editing and periodic orbit extraction using morse decomposition. *IEEE Trans. Vis. Comp. Graph. 13*, 4, 769–785.

COHEN-STEINER, D., AND MORVAN, J. 2003. Restricted delaunay triangulations and normal cycle. In *Proc. ACM Symp. Comp. Geom.*, 312–321.

DELMARCELLE, T., AND HESSELINK, L. 1994. The topology of symmetric, second-order tensor fields. *IEEE Computer Graphics and Applications*, 140–147.

DONG, S., KIRCHER, S., AND GARLAND, M. 2005. Harmonic functions for quadrilateral remeshing of arbitrary manifolds. *CAGD*, 5, 392–423.

DONG, S., BREMER, P.-T., GARLAND, M., PASCUCCI, V., AND HART, J. C. 2006. Spectral surface quadrangulation. *ACM Trans. Graph. 25*, 3, 1057–1066.

FISHER, M., SCHRÖDER, P., DESBRUN, M., AND HOPPE, H. 2007. Design of tangent vector fields. *ACM Trans. Graph. 26*, 3, 56.

GIRSHICK, A., INTERRANTE, V., HAKER, S., AND LEMOINE, T. 2000. Line direction matters: an argument for the use of principal directions in 3D line drawings. *Proc. NPAR*, 43–52.

GU, X., HE, Y., JIN, M., LUO, F., QIN, H., AND YAU, S.-T. 2007. Manifold splines with single extraordinary point. In *ACM SPM*, 61–72.

HAMILTON, R. S. 1982. Three-manifolds with positive ricci curvature. *J. Diff. Geom. 17*, 255–306.

HELMAN, J. L., AND HESSELINK, L. 1991. Visualizing vector field topology in fluid flows. *IEEE CG&A 11* (May), 36–46.

HERTZMANN, A., AND ZORIN, D. 2000. Illustrating smooth surfaces. *Proc. ACM/SIGGRAPH Conf.* (Aug.), 517–526.

JIN, M., KIM, J., LUO, F., AND GU, X. 2007. Discrete surface ricci flow: Theories and applications. In *Mathematics of Surfaces XII*, Springer, vol. 4647 of *Lecture Notes in Computer Science*, 209–232.

KÄLBERER, F., NIESER, M., AND POLTHIER, K. 2007. Quadcover - surface parameterization using branched coverings. *Comp. Graph. Forum 26*, 10 (Sep), 375–384.

KAPLAN, M., AND COHEN, E. 2003. Computer generated celtic design. In *Proceedings of the 14th Eurographics Workshop on Rendering Techniques*, 2–19.

KHAREVYCH, L., SPRINGBORN, B., AND SCHRÖDER, P. 2006. Discrete conformal mappings via circle patterns. *ACM Trans. Graph. 25*, 2, 412–438.

LIU, Y., LIN, W.-C., AND HAYS, J. 2004. Near-regular texture analysis and manipulation. *ACM Trans. Graph. 23*, 3, 368–376.

MARINOV, M., AND KOBBELT, L. 2004. Direct anisotropic quad-dominant remeshing. *Proc. Pacific Graph.*, 207–216.

MEYER, M., DESBRUN, M., SCHRÖDER, P., AND BARR, A. H. 2002. Discrete differential-geometry operators for triangulated 2-manifolds. *VisMath*.

NI, X., GARLAND, M., AND HART, J. C. 2004. Fair morse functions for extracting the topological structure of a surface mesh. *ACM Trans. Graph. 23*, 3, 613–622.

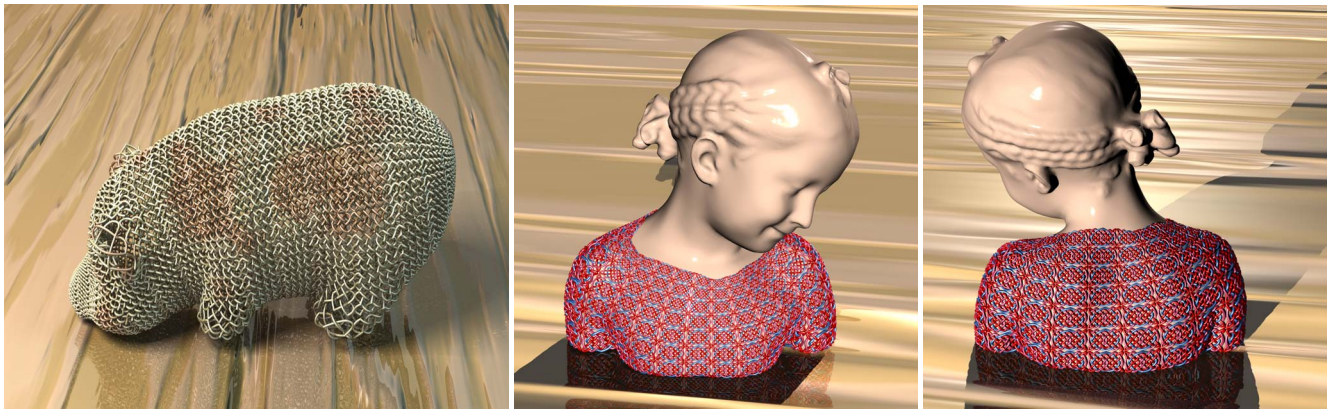

**Figure 16: Celtic knots designed surfaces** .


PALACIOS, J., AND ZHANG, E. 2007. Rotational symmetry field design on surfaces. *ACM Trans. Graph. 26*, 3, 55.

PRAUN, E., FINKELSTEIN, A., AND HOPPE, H. 2000. Lapped textures. *Proc. ACM/SIGGRAPH Conf.* (Aug.), 465–470.

RAY, N., LI, W. C., LÉVY, B., SHEFFER, A., AND ALLIEZ, P. 2006. Periodic global parameterization. *ACM Trans. Graph. 25*, 4, 1460–1485.

RAY, N., VALLET, B., LI, W.-C., AND LEVY, B. to appear. N-symmetry direction field design.

RUSINKIEWICZ, S. 2004. Estimating curvatures and their derivatives on triangle meshes. In *Proc. 3DPVT*, 486–493.

STAM, J. 2003. Flows on surfaces of arbitrary topology. *Proc. ACM/SIGGRAPH Conf. 22*, 3 (July), 724–731.

TARINI, M., HORMANN, K., CIGNONI, P., AND MONTANI, C. 2004. Polycube-maps. *ACM Trans. Graph. 23*, 3, 853–860.

THEISEL, H. 2002. Designing 2d vector fields of arbitrary topology. In *Proc. Eurographics*, vol. 21, 595–604.

TONG, Y., ALLIEZ, P., COHEN-STEINER, D., AND DESBRUN, M. 2006. Designing quadrangulations with discrete harmonic forms. *Proc. Symp. Geom. Proc.*, 201–210.

TURK, G. 2001. Texture synthesis on surfaces. In *Proc. ACM/SIGGRAPH Conf.*, 347–354.

VAN WIJK, J. J. 2002. Image based flow visualization. *Proc. ACM/SIGGRAPH Conf. 21*, 3 (July), 745–754.

VAN WIJK, J. J. 2003. Image based flow visualization for curved surfaces. *Proc. IEEE Vis.* (Oct), 123–130.

WEI, L. Y., AND LEVOY, M. 2001. Texture synthesis over arbitrary manifold surfaces. *Proc. ACM/SIGGRAPH Conf.*, 355–360.

ZELINKA, S., AND GARLAND, M. 2004. Jump map-based interactive texture synthesis. *ACM Trans. Graph. 23*, 4, 930–962.

ZHANG, E., MISCHAIKOW, K., AND TURK, G. 2006. Vector field design on surfaces. *ACM Trans. Graph. 25*, 4, 1294–1326.

ZHANG, E., HAYS, J., AND TURK, G. 2007. Interactive tensor field design and visualization on surfaces. *IEEE TVCG 13*, 1, 94–107.

ZHOU, K., HUANG, X., WANG, X., TONG, Y., DESBRUN, M., GUO, B., AND SHUM, H.-Y. 2006. Mesh quilting for geometric texture synthesis. *ACM Trans. Graph. 25*, 3, 690–697.


## Appendix

**Theorem 3.1** *Suppose* $\mathbf{v}$ *is a smooth vector field on a surface* $M$ *with an initial metric* $\mathbf{g}(0)$. $\mathbf{g}(t)$ *is a one parameter family of Riemannian metric tensors. Then for any closed loop* $\gamma$ *on* $M$*, the relative rotation* $T_{\mathbf{v}}(\gamma)$ *on* $(M, \mathbf{g}(t))$ *is a constant for any* $t$.

*Proof* The Levi-Civita connections are continuously determined by $\mathbf{g}(t)$, therefore the parallel transportation is continuously determined by $\mathbf{g}(t)$. The absolute rotation of $\mathbf{v}$ along $\gamma$, $R_{\mathbf{v}}(\gamma)$ is a continuous function of $t$, and so is the holonomic rotation of $\gamma$, $h(\gamma)$. We have that the relative rotation $T_{\mathbf{v}}(\gamma)$ is a continuous function. Because $\mathbf{v}$ is smooth on $(M, \mathbf{g}(0))$, therefore $\frac{N}{2\pi} T_{\mathbf{v}}(\gamma)|_{t=0}$ is an integer. Because it is also continuous, therefore, it must be a constant for all $t$. Because $\gamma$ is arbitrary, therefore the homotopy type of $\mathbf{v}$, the indexes of the singularities are preserved during the continuous metric deformation $\mathbf{g}(t)$. Q.E.D.

**Theorem 3.2** *Suppose* $M$ *is a surface with a flat cone metric. A parallel n-RoSy field exists on the surface, if and only if all the holonomic rotation angles of the metric are integer times of* $\frac{2\pi}{n}$.

*Proof* If the holonomic rotations of the flat cone metric are $\frac{2k\pi}{N}$, then parallel transporting an N-RoSy at the base point results in a field $\mathbf{v}$, $R_{\mathbf{v}}(\gamma) = 0$ for any loop $\gamma$. Consequently the compatibility is satisfied and the field is smooth. Reversely, if there exists a smooth parallel N-RoSy field $\mathbf{v}$, then $R_{\mathbf{v}}(\gamma)$ is zero for any loop $\gamma$. Therefore, $h(\gamma)$ must be integer times of $\frac{2\pi}{N}$. Q.E.D.

**Corollary 3.3** *Suppose* $M$ *is a genus zero closed surface with a finite number of cone singularities.* $M$ *has a parallel N-RoSy field, if and only if the curvature for each cone singularity is* $\frac{2k\pi}{N}$.

*Proof* Let $\gamma$ be a loop, which is the boundary of a region $\Omega$ on the surface. Suppose there are $m$ cone singularities $\{s_1, s_2, \cdots, s_m\}$ inside $\Omega$. According to Gauss-Bonnet theorem, the holonomic rotation angle of $\gamma$ equals to the total curvature of $\Omega$, $h(\gamma) = \sum_{i=1}^{m} k_i$, where $k_i$ is the curvature of $s_i$. Let $\gamma_i$ be a loop surrounding $s_i$ without enclosing any other singularities, then $\{\gamma_i, i = 1, 2, \cdots, m-1\}$ is a set of generators of $\pi(\bar{M})$. $M$ has a smooth parallel N-RoSy field, if and only if all $h(\gamma_i)'s$ are $\frac{2k\pi}{N}$. Q.E.D.

**Theorem 3.4** *Suppose* $M$ *is a surface with flat cone metric, then there exists a smooth N-RoSy field.*

*Proof* There exists a unique harmonic 1-form $\omega$, such that $\int_\gamma \omega = h(\gamma)$, for any loop $\gamma$ on $\bar{M}$. We parallel transport an N-RoSy from the base point, and rotate it during the transportation by an angle $\int_\gamma \omega$, where $\gamma$ is any path from the base to the current point. The resulting field is smooth. Q.E.D.

**Theorem 3.5** *Suppose* $M$ *is with a flat cone metric, the holonomy group of* $\bar{M}$ *is* $H(\bar{M})$*, if* $H(\bar{M})$ *is a subgroup of* $G_T$*, then* $T$ *can be defined on* $M$.

Proof Let $\tilde{M}$ be the universal covering space of $\bar{M}$. We equip $\tilde{M}$ with the flat cone metric and immerse $\tilde{M}$ onto the plane $\mathbb{R}^2$. Then the deck transformation group is a subgroup of the holonomy group $H(\bar{M})$. If $T$ is a tessellation on $\mathbb{R}^2$, it is invariant under the action of $G$. $H(\bar{M})$ is a subgroup of $G$, so is the deck transformation group. Therefore, $T$ is invariant under all the deck transformations of $\tilde{M}$, and so $T$ can be defined on $\bar{M}$. Q.E.D.

For a mesh with a flat cone metric, homotopic loops have the same holonomy. It can be further proved that homologic loops have the same holonomy. But only homotopy loops have the same generalized holonomy. For the sake of simplicity, we don't introduce the concept of homology.